WPMST1-PR(17) 17965

M. Gobbin et al.

Role of plasma response to applied magnetic perturbations in runaway electron mitigation in tokamaks

Preprint of Paper to be submitted for publication in
Physical Review Letters

This work has been carried out within the framework of the EUROfusion Consortium and has received funding from the Euratom research and training programme 2014-2018 under grant agreement No 633053. The views and opinions expressed herein do not necessarily reflect those of the European Commission.

This document is intended for publication in the open literature. It is made available on the clear understanding that it may not be further circulated and extracts or references may not be published prior to publication of the original when applicable, or without the consent of the Publications Officer, EUROfusion Programme Management Unit, Culham Science Centre, Abingdon, Oxon, OX14 3DB, UK or e-mail Publications.Officer@euro-fusion.org

Enquiries about Copyright and reproduction should be addressed to the Publications Officer, EUROfusion Programme Management Unit, Culham Science Centre, Abingdon, Oxon, OX14 3DB, UK or e-mail Publications.Officer@euro-fusion.org

The contents of this preprint and all other EUROfusion Preprints, Reports and Conference Papers are available to view online free at http://www.euro-fusionscipub.org. This site has full search facilities and e-mail alert options. In the JET specific papers the diagrams contained within the PDFs on this site are hyperlinked

Role of plasma response to applied magnetic perturbations in runaway electron mitigation in tokamaks

M.Gobbin[1], L.Li[2], Y.Q.Liu[3], L.Marrelli[1], M.Nocente[4], G.Papp[5], G.Pautasso[5], P.Piovesan[1], M.Valisa[1], P.J.McCarthy[6], P.Martin[1], W.Suttrop[5], M.Teschke[5], the ASDEX Upgrade Team[5] and the EUROfusion MST1 Team*
[1] *Consorzio RFX, Padova (CNR, ENEA, INFN,Universitá di Padova, Acciaierie Venete SpA)- Italy*
[2] *College of Science, Donghua University, Shanghai, Peoples Republic of China*
[3] *General Atomics, San Diego, CA 92186-5608, USA*
[4] *Dipartimento di Fisica, Universitá di Milano-Bicocca, Milano, Italy*
[5] *Max-Planck-Insitute for Plasma Physics, Garching, Germany*
[6] *Department of Physics, University College Cork, Cork, Ireland and*
∗*see H. Meyer et al., Nuclear Fusion FEC 2016 Special Issue (2017)*

Runaway electrons generated during disruption events represent a severe threat for plasma-facing components in controlled fusion devices and require reliable and efficient mitigation techniques. The application of resonant magnetic perturbations (RMPs) in the ASDEX Upgrade experiment results in a lower amount and duration of the post-disruption runaway electron current with a partial decrease of the associated hard-X-ray energy. The efficacy of this technique strongly depends on the poloidal spectrum of the perturbations evaluated including the plasma response to RMPs. These findings are likely to be of general interest as a tool to limit the negative effects of runaway electrons in larger fusion devices like ITER.

Suprathermal electrons moving in a plasma experience a friction force decreasing with their velocity and, when a sufficiently strong electric field is applied, a certain fraction of them may undergo a runaway process i.e. they can be continuously accelerated up to velocities close to the speed of light [1, 2]. The physics of high energy electrons and of their interaction with magnetic fields has been investigated in a large variety of phenomena, ranging from the Earth's atmosphere [3, 4] and magnetosphere [5], to the solar corona - where fast particle beams are generated during magnetic reconnection events [6] - and more generally in astrophysics [7–9]. Runaway electrons (RE) are also known to occur in laboratory plasmas and represent one of the outstanding problems for fusion devices in the tokamak configuration [10] and in particular for future operations in the international experimental reactor ITER [11] currently under construction in the south of France. Indeed, runaway electrons are often generated during disruptions [12–14], events that involve the fast deposition of the stored thermal energy on plasma-facing components. The sudden cooling of the plasma and the subsequent increase of its resistivity leads to a fast growth of the toroidal electric field that, above a critical threshold E_c ($\approx 0.8 n_{e,20}$, with $n_{e,20}$ the electron density in $10^{20} m^{-3}$ and E_c in V/m), generates primary runaway electrons [15, 16]. Such a seed of fast electrons, in turn, may produce more runaways by forward momentum transfer to thermal electrons and so forth in a cascade process (secondary RE generation or the avalanche mechanism). In high plasma current ($\sim$ 10 MA) and larger devices like ITER the secondary RE generation is expected to be dominant and produce several orders of magnitude more runaways than in current experiments [17] with energies exceeding $\sim$ 100 MeV [18–20]; hence, an adequate protection plan for ITER can hardly be extrapolated and validated in existing tokamaks. The occurrence of such energetic particle beams represents a severe risk since they can strike and seriously damage the surrounding structures through their highly localized energy deposition. The prevention and mitigation of their harmful effects is thus of paramount importance for safe operations and to ensure a long life to a commercial reactor.

At present, in order to prevent or limit such a RE generation, the main solution is the dissipation of the energy of fast electrons via Coulomb scattering by increasing the density. Several techniques directed to this end are extensively investigated in the tokamak community, for instance Massive Gas Injection (MGI) [21–25] and shattered pellet injection [28, 29]. Also, the interaction of non-axisymmetric magnetic fields - spontaneously generated by the plasma or applied by external coils - with the fast particle population might represent a possible tool for RE mitigation [30, 31] as tested in existing devices [32–36] and examined with numerical simulations dedicated to ITER scenarios [37–39]. In these experiments, resonant magnetic perturbations (RMPs) [40] could decrease the post-disruption RE current with an efficiency depending on the amplitude of the RMPs; these findings have been mainly interpreted in terms of RE deconfinement due to ergodization. Nevertheless, a systematic suppression of runaway electrons has not yet been achieved [33] and also the results obtained from RMPs with different toroidal/poloidal wave numbers [34] require further investigation.

A major and innovative contribution to these studies comes from the experiments recently performed in the medium size tokamak ASDEX Upgrade [41, 42] reported in this Letter. RMPs applied by external coils [43] before the disruption significantly reduce the current and lifetime of the resulting RE beams with a strength depending on the perturbation poloidal spectrum. Here, such a phenomenology is explained by evaluating the total radial magnetic field taking into account the plasma

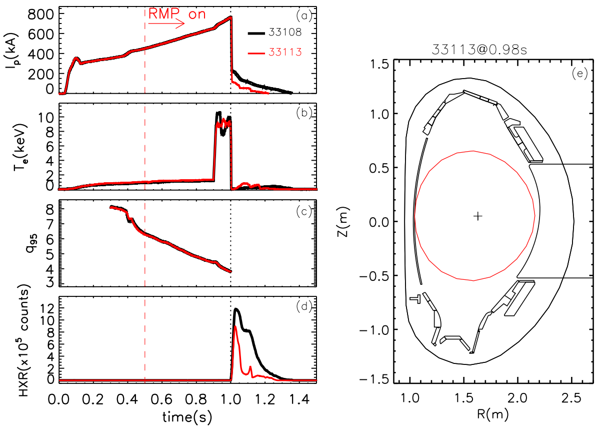

FIG. 1: Evolution of (a) plasma current, (b) core electron temperature, (c) safety factor at the edge, (d) HXR emission for two different shots: in black for a standard one (no mitigation methods used), in red for a discharge where RMPs by the B-coils are applied from $t = 0.5$ s (vertical dashed line). The dashed vertical black line at 1 s corresponds to the time of disruption. In panel (e) the equilibrium reconstruction for the last closed surface of shot 33113 at 0.98 s.

response [44] to the RMPs i.e. the capability of a plasma, close to marginal stability, to amplify magnetic perturbations and hence to experience significant helical deformations. Indeed, as shown in the following, a vacuum approximation fails in the interpretation of the experimental data. These results, presented here for the first time, are general and relevant also for other existing and future tokamak devices.

Experimental setup and results. The ASDEX Upgrade scenario for these experiments is based on a discharge with toroidal magnetic field $B_T = -2.5$ T, plasma current of $I_p = 800$ kA and central electron density in the range $2.5 - 3.5 \cdot 10^{19}$ m^{-3} [25, 45]. The plasma is circularly shaped (Fig.1-(e)), limited by the inner wall; a power of 2.5 MW of Electron Cyclotron Resonance Heating (ECRH) is applied for 100 ms from $t = 0.9$ s to heat the plasma and introduce a fast particle seed just before the disruption, which is triggered by the injection of Argon gas. Fig.1 shows with black lines the main waveforms of the standard discharge evolution when no mitigation methods are used; the plasma current I_p is ramped till $t = 1$ s, when the disruption is induced. Then, part of I_p is converted into runaway beam current (I_{RE}) with an initial value of ~ 200 kA decreasing to zero in about 0.35 s. The central electron temperature measured by the Electron Cyclotron Emission diagnostic grows from 1 to $\sim 10 - 12$ keV during the ECRH heating and collapses at 1 s in less than 1 ms (thermal quench phase, in panel (b)). The safety factor ($q = aB_T/B_PR_0$ with B_T,B_P the toroidal and poloidal field respectively and a,R_0 the minor and major radius of the plasma) near the plasma boundary (q_{95}, i.e q at 95% of the minor radius a) decreases from 8 to a value close to 4 just before the disruption, as shown in panel (c). Finally, Hard X-Ray (HXR) measurements from a scintillator diagnostic [26, 27] are reported in the last panel; they are greater than zero only in the post-disruption phase with a temporal evolution similar to the I_{RE} in panel (a).

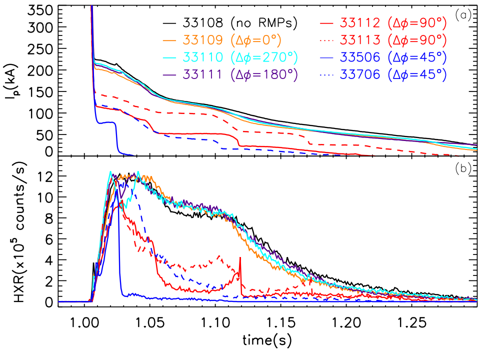

FIG. 2: (a) Plasma current during the post disruption phases for different values of $\Delta\Phi$ and (b) corresponding HXR emission.

ASDEX Upgrade is equipped with a set of sixteen non-axisymmetric in-vessel coils [46] in the form of two toroidal rows of eight coils (termed B-coils) above and below the tokamak midplane on the outer side of the torus (low field side). They were powered by four independent power supplies which produce a radial field of $\sim 10^{-4}$ T at the plasma boundary in front of an upper coil ($b^r/B_T \sim 10^{-4}$). The B-coils can generate resonant magnetic perturbations with dominant toroidal mode numbers $n = 1, 2, 4$. The poloidal mode number spectrum m is defined by the poloidal dimension of the coils and their reciprocal distance; generally there is no single corresponding m, but a broad spectrum of modes and harmonics. The differential phase $\Delta\Phi$ between the current harmonic flowing in the upper (I_{upper}) and lower (I_{lower}) set of coils can be modified in order to change the alignment of the perturbation field with respect to the equilibrium magnetic field lines. The differential phase $\Delta\Phi$ is defined through the following relations: $I_{\text{upper}} \propto \cos(n\phi_{\text{coil}})$ and $I_{\text{lower}} \propto \cos(n\phi_{\text{coil}} + \Delta\Phi)$ where ϕ_{coil} is the toroidal angle location of the center of a B-coil.

In the experiments reported in this paper $\Delta\Phi$ steps of 45° are performed and the perturbations generated are characterized by a dominant $n = 1$ toroidal mode number; the B-coils carry a maximum current of $I_B = 1$ kA and are turned on 500 ms before the disruption, at $t = 0.5$ s. An example of discharge with magnetic perturbations applied with $\Delta\Phi = 90°$ is shown in Fig.1 (red colour). Panel (a) shows that both the initial runaway current and the beam duration in the post-disruption phase are almost halved with respect to the unmitigated RE discharge without external field application. Similarly, the HXR signal decreases by a factor of $\sim 2 - 3$ in less than

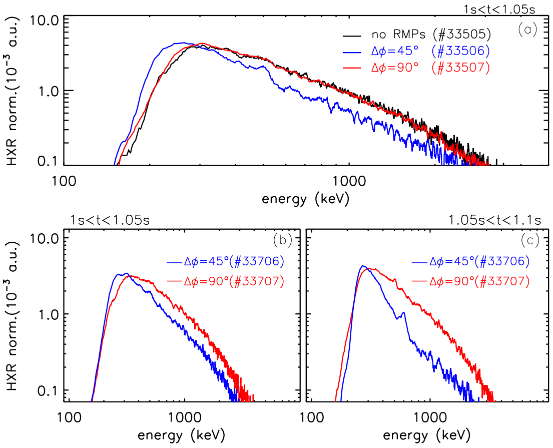

FIG. 3: (a): HXR energy spectrum from a scintillator diagnostic for standard shot (black) and for two with RMPs applied but with different $\Delta\Phi$ (45°- blue curve and 90°- red curve). (b)-(c): HXR energy spectra reconstruction in two different time intervals after the disruptions for shots with RMPs applied (45°- blue curve and 90°- red curve).

50 ms, and remains close to zero afterwards.
The phenomenology observed above is present only for specific differential phases of the B-coils. A scan in $\Delta\Phi$ was performed and the final currents and HXR measurements during the RE beam phase are reported in Fig.2. No significant effect of the applied perturbation is visible for $\Delta\Phi = 0°, 180°$ and $270°$. However, both the discharges reported in this plot with $\Delta\Phi = 90°$ are characterized by a reduction of the RE current ($\sim -40\%$) and HXR emission ($\sim -60\%$). This behaviour is even more pronounced for $\Delta\Phi = 45°$, where the runaway beam, with an initial current much lower than in the other discharges ($\sim$ 70 kA), is suppressed in less than $30ms$. RMPs slightly increase the edge electron density when applied in the pre-disruption phase, regardless of the value of $\Delta\Phi$ and of the initial RE beam current. Thus the mitigation effect of RMPs on runaways is not a mere consequence of different density regimes induced by the applied perturbations before the disruption.

Effect of RMPs on HXR energy spectrum. Magnetic perturbations also affect the energy of the HXRs emitted by runaway electrons. Three examples of HXR spectra, normalized to the total number of events, are reported in Fig.3-(a) in the time interval between 1 and $1.05s$ (just after the disruption): the black curve refers to a standard discharge (no RMP applied), while the red and blue ones to perturbed shots ($\Delta\Phi = 90°$ and $45°$, respectively). By analyzing the slope of these distributions it is found that the 45° trace falls off clearly faster in the range $300 - 600$ keV, with the exception of a quasi constant region between 400 and 500 keV which is of comparable shape also in the 90° discharge. These variations in the HXR spectrum, when different $\Delta\Phi$ are applied, qualitatively reflect the changes in the RE energy distribution. A more detailed determination of the RE energy requires dedicated methods [47] and modeling activity is currently in progress. Other examples are reported in Fig.3-(b)-(c): the normalized HXR spectra of shots with $\Delta\Phi = 45°, 90°$ are evaluated just after the disruption ((b), $1s < t < 1.05s$) and between $1.05s$ and $1.1s$ (c). In the latter time interval the slope of the distribution relative to the $\Delta\Phi = 45°$ discharge in the energy range $300 - 800keV$ becomes steeper by $\sim 60\%$ with respect to the one in panel (b). Such a result is of great relevance since it highlights a possible effect of the RMPs also during the RE beam phase if applied with the appropriate differential phase. On the contrary, the spectrum for the $\Delta\Phi = 90°$ case does not show a similar variation between the two time intervals considered. The distinctive behavior of the phase $\Delta\Phi = 45°$ with respect to others will be discussed in the next section.
Role of plasma response in RE mitigation. The poloidal spectrum of the applied 3D fields has been evaluated in vacuum approximation at the time $t = 0.98s$, just before the disruption event, for more differential phases of the B-coils. Two examples are shown in panels (a)-(b) of Fig.4 as function of the poloidal wave number m and of the normalized poloidal flux coordinate (ρ_{pol}) for $\Delta\Phi = 45°$ and $\Delta\Phi = 315°$, respectively. The safety factor profile is plotted with a white dotted line and the resonant positions corresponding to $q = 3$ and $q = 4$ are marked with dots. The $\Delta\Phi = 45°$ case shows that the maximum perturbed field occurs in the edge region and between the non-resonant component $m = 5$ and $m = 6$; the resonant position with $q = 4$ on the other hand lies in a region of low field ($<$ 1.5 G). By increasing the B-coil phase difference, such a maximum is continuously shifted to lower values of m and at $\Delta\Phi = 315°$ intersects the region with the rational surfaces $q = 3$ and $q = 4$ (Fig.4-(b)). As the parameter to quantify the variation of the RMP amplitude b_r with $\Delta\Phi$, the value of the $m = 4$ perturbed field component at the resonance $q = 4$ was evaluated and shown in Fig.5(a) with a black-dotted line. As clear from this plot, the $n = 1$ radial field resonant with $q = 4$ (in the vacuum approximation) is maximum when $\Delta\Phi \sim 315°$ with a minimum value close to zero around $\Delta\Phi \sim 100°$; a similar trend is found also for the $m = 3$ mode estimated at $q = 3$ position (not shown in the figure for the sake of clarity). Such a dependence cannot explain the experimental data described in the previous sections summarized in Fig.5; panel (b) and (c) respectively show the initial RE post-disruption current and the duration of the RE beam (estimated as the interval from the disruption to the time when $I_{RE} < 10$ kA). Here, each point corresponds to a different discharge and the dashed line to the average post-disruption current for shots where RMPs are not applied. For the two shots with $\Delta\Phi = 45°$ the initial runaway electron beam current is reduced by more than a factor of 2; also the RE beam duration is similarly affected and decreases to a few tens of ms for one of these discharges. A similar effect is found when $\Delta\Phi = 90°$. No RE mitigation is observed for $\Delta\Phi \sim 315°$ where RMPs give the largest

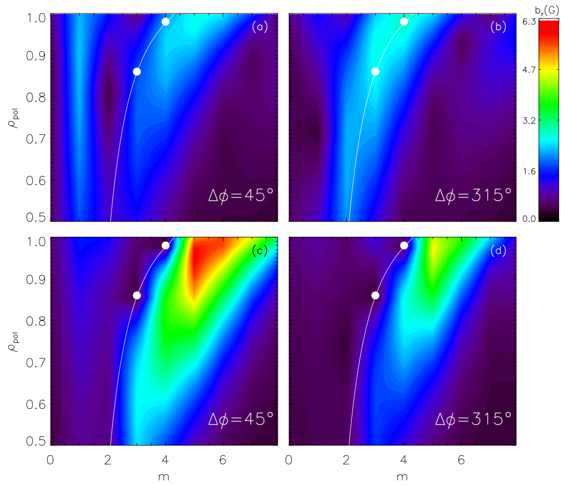

FIG. 4: Contour of perturbed field function of the m component and normalized poloidal flux for two values of the B-coil differential phase with (a) 45° and (b) 315° in vacuum approximation while (c) 45° and (d) 315° including the plasma response.

contribution to the resonant position at $q = 4$ (or $q = 3$) in the vacuum approximation.

The code MARS-F [48, 49], which solves the single-fluid linearly perturbed MHD equations in full toroidal geometry, has been used to calculate the poloidal spectrum including the plasma response to RMPs. Fig.4-(c) and (d) show the results obtained for $\Delta\Phi = 45°$ and 315° relative to an equilibrium preceding the disruption (reference shot: 33113, $t = 0.98$ s); the corresponding kinetic quantities such as electron/ion temperature and density profiles are provided by Integrated Data Analysis (IDA) [50] of diagnostics. In these simulations a toroidal rotation of $\omega/\omega_A = 5 \cdot 10^{-3}$ is assumed (ω_A is the Alfvén frequency for the considered plasmas). In both cases, the plasma response reduces the amplitude of resonant harmonics at the corresponding rational surfaces compared with the vacuum field; on the other hand the kink relative to the components $m = 5, 6$ for $\Delta\Phi = 45°$ is enhanced by more than a factor 3. The same analysis has been performed for more $\Delta\Phi$ and toroidal rotation values.

As for the vacuum field, the $m = 4$ resonant component at $q = 4$ is shown in Fig.5-(a) with red squares; its amplitude is reduced by a factor ~ 8 with respect to the vacuum approximation. The differential phase relative to the maximum is shifted by $\sim 45° - 60°$ in the direction of increasing $\Delta\Phi$ values, thus closer to the B-coil differential phase experimentally more successful in reducing the RE beam current. The same panel reports also the average amplitude of the non resonant mode $m = 5$ (blue-triangles curve) in the edge region ($\rho_{pol} > 0.8$). A clear maximum can be observed at $\Delta\Phi \sim 45° - 90°$ with an absolute value higher than 5 G; the RMP configuration for which runaway electrons are best mitigated is thus related to the largest edge kink response. A similar behavior was found for the B-coil configuration most efficient in suppressing edge localized modes (ELMs) [51, 52], where the maximum field evaluated including the plasma response is offset $\sim 60°$ from the one in vacuum approximation [53]. The results presented here do not depend on the toroidal rotation if ω/ω_A is between 10^{-3} and $5 \cdot 10^{-3}$. An estimate of the experimental toroidal flow can be inferred from the rotation frequency of the inner $n = 1$ mode when present and is of the order of ~ 5 kHz ($\omega/\omega_A \sim 2 \cdot 10^{-3}$).

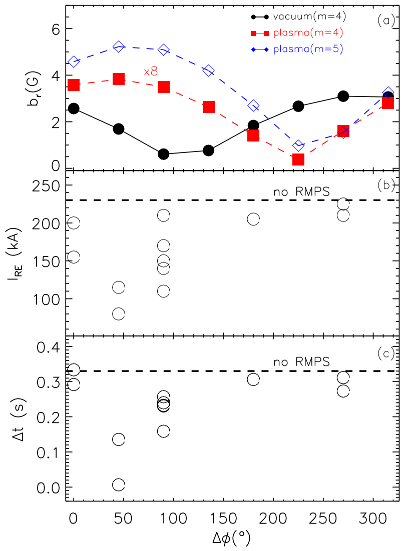

FIG. 5: (a) Perturbed field amplitude at the resonance $q = 4$ and of the kink mode $n = 5$ in the edge region, (b) post-disruption RE current and (c) RE beam duration. The dotted line corresponds to the average RE current in standard discharges.

The total perturbed field (vacuum + plasma response) of the resonant field components is relevant in the formation of magnetic islands (e.g. harmonics (4, 1) and (3, 1)) and, potentially, can be responsible for field line ergodization. But also the non-resonant part (kink amplification), that does not necessarily ergodize fields, further contributes to RE suppression (by coupling to resonant spectrum or direct orbit modification). In this sense, the combined results reported in Figure 4-5 point to two mechanisms both occurring at the same favorable coil phasing which could affect the primary generated runaway electrons, thus reducing the initial seed, or those produced in the avalanche process. Nevertheless, a deeper understanding of these issues would require a detailed analysis directly by modeling the RE trajectories in these 3D fields [54] and/or an investigation with a two-fluid approach [55], considering also non-linear effects in the plasma response to RMPs. When two-fluid terms are included in the response calculations, the ion and electron velocity are no longer the same; in particular the electron velocity results to be the relevant quantity controlling the field penetration in the core of the plasma at the mode-rational surface. Conversely, the excitation of edge modes is mainly correlated with the ion velocity [56]. Such an analysis, which is beyond the scope of this work, might contribute to determine the necessary and sufficient conditions for the development of magnetic islands and of stochasticity.

Conclusions. The application of RMPs in the ASDEX Upgrade experiment results in a significantly reduced current and lifetime of the generated RE beam. A similar effect is observed also in the hard-x-ray spectrum characterized by a partial decrease of the high energy content. These findings are strongly dependent on the poloidal spectrum of the applied RMPs when the plasma response is included in the analysis by the code MARS-F. Indeed, the modest amplification (factor of $2-3$) of the edge kink response, with respect to a crude vacuum approximation, has to be considered to explain the observed suppression effects. These results can contribute to explain similar experiments performed in other tokamak devices and - combined with disruption predictive models [57–60] and in synergy with standard mitigation methods - be relevant for RE suppression in future fusion reactors.

Acknowledgments. This work has been carried out within the framework of the EUROfusion Consortium and has received funding from the Euratom research and training programme 2014-2018 under grant agreement No 633053. The views and opinions expressed herein do not necessarily reflect those of the European Commission. Work supported by US DoE Office of Science under Contract DE-FG02-95ER54309 and DE-FC02-04ER54698.

[1] R.M. Kulsrud *et al.* Phys. Rev. Lett. **31**, 690 (1973)
[2] H.Dreicer *et al.*, Phys.Rev **117**, 329 (1960)
[3] B.E.Carlson *et al.* Journal of Geophysical Research, **113**, A10307 (2008)
[4] A.V. Gurevich *et al.*, Radio Science **31**, 1541 (1996)
[5] N.G.Lehtine *et al.* Geophysical Research Letters, **27**, 1095 (2000)
[6] J.Stepan *et al.* Astronomy & Astrophysics **472**, L55 (2007)
[7] E. Moghaddam-Taaheri and C.K. Goertz, Astrophysical Journal, **352**, 361 (1990)
[8] J.S.Kaastra, Journal of Plasma Physics **29**, 287 (1983)
[9] M.J.Houghton, Planetary and Space Science, **23**, 409 (1975)
[10] Wesson, J. Tokamaks 3rd edn, Ch. 13, 711717 (Oxford Univ. Press, Oxford, 2004).
[11] The ITER physics basis. Nucl. Fusion **47**, S1-S413 (2007).
[12] Hender T. C. *et al.* Nucl. Fusion **47**, S128202 (2007)
[13] E.C.Hollmann *et al.* Phys.Plasmas **22**, 056108 (2015)
[14] M. Lehnen *et al.* JNM **463** 39 (2015)
[15] J. W. Connor and R. J. Hastie, Nucl. Fusion **15**, 415424 (1975).
[16] R.S.Granetz *et al.* Phys. Plasmas **21**, 072506 (2014)
[17] A.H.Boozer Nucl. Fusion **57** (2017) 056018
[18] Hender T.C. *et al.* , The ITPA HD, Disruption and Magnetic Control Topical Group 2007 Nucl. Fusion **47** S128
[19] M.N.Rosenbluth and S.V.Putvinski, Nucl.Fusion **37**, 1355 (1997)
[20] R.Aymar, *et al*, Plasma Phys. Control. Fusion **44**, 519 (2002)
[21] Bakhtiari M. *et al* Nucl. Fusion **42**, 1197 (2002)
[22] S. A. Bozhenkov *et al* Plasma Phys. Control. Fusion **50**, 105007 (2008)
[23] C.Reux *et al*, Nucl. Fusion **50**, 095006 (2010)
[24] Z. Y. Chen, Plasma Phys. Control. Fusion **55**, 014046 (2017)
[25] G.Pautasso *et al*, Plasma Phys. Control. Fusion **59**, 035007 (2016)
[26] M.Nocente *et al* Rev. Sci. Instrum. **81**, 10D321 (2010)
[27] M.Nocente *et al* IEEE Trans. Nucl. Sci. **60** 1408 (2013)
[28] Taylor P.L. *et al* Phys. Plasmas **6**, 1872 (1999)
[29] N.Commaux *et al* Nucl. Fusion **51**, 103001 (2011)
[30] P.Helander *et al* Phys.Plasmas **7**, 4106 (2000)
[31] R.W.Harvey *et al*, Phys. Plasmas **7**, 4590 (2000)
[32] M.Lehnen *et al*, Phys.Rev.Lett. **100**, 255003 (2008)
[33] K. Wongrach1 *et al* Nucl. Fusion **55**, 053008 (2015)
[34] Hollmann E.M. *et al* Phys. Plasmas **17** 056117 (2010)
[35] R.Yoshino *et al*, Nucl.Fusion **40**, 1293 (2000)
[36] M.Gobbin *et al.* Nucl. Fusion **57**, 016014 (2017)
[37] G.Papp *et al.* Journal of Plasma Physics **81** 47581050 (2015)
[38] G.Papp *et al.* Plasma Physics and Controlled Fusion, **54** (2012)
[39] K.Aleynikova *et al.*, P. Plasma Phys. Rep. **42**, 486 (2016)
[40] T.Evans *et al.*, Phys. Rev. Lett. **92**, 235003 (2004)
[41] A. Herrmann Fusion Sci. Technol. **44**, 569 (2003)
[42] A.Kallebanch *et al.* to be published on Nuclear Fusion (IAEA 2016)
[43] W.Suttrop *et al.*. Phys. Rev. Lett. **106** 225004 (2011)
[44] Y.Q.Liu *et al.* Nucl. Fusion **51** (2011)
[45] G.Papp *et al.* to be published in Nuclear Fusion (IAEA 2016)
[46] Conway et al. Plasma Phys.Control.Fusion **57** (2015)
[47] A.E. Shevelev *et al* Nucl. Fusion **53** (2013) 123004
[48] Y.Q.Liu *et al.* Phys. Plasmas **7** 3681 (2000)
[49] Y.Q.Liu *et al.* Phys. Plasmas **17** 122502 (2010)
[50] R.Fischer *et al.* Fusion Sci. Technol.**58** 675 (2010)
[51] F.Orain *et al.* Nucl. Fusion **57** 022013 (2017)
[52] L.Li *et al.* Nucl. Fusion **56**, 126007 (2016)
[53] D.A.Ryan *et al.* Plasma Phys. Control. Fusion **57** 095008 (2015)
[54] K. Sarkimaki *et al.* Plasma Phys. Control. Fusion **58** 125017 (2016)
[55] F.Orain *et al.* 2013 Physics of Plasmas **20**, 102510 (2013)
[56] N.M. Ferraro, Phys.Plasmas **19**, 056105 (2012)
[57] G. A. Rattá, *et al.*, Nuclear Fusion **50** 025005 (2010)
[58] G.Pautasso *et al.*, Nuclear Fusion **51** 103009 (2011).
[59] S. Dormido-Canto *et al.*, Nuclear Fusion **53** 113001 (2013).
[60] P. De Vries *et al* Nuclear Fusion **56** 2 (2016)